Transparent Magnesium Hydroxide/Acrylate Nanocomposite Films

S. Wriedt, S. Kaskel

Department of Inorganic Chemistry, Technical University of Dresden, Dresden 01069, Germany

ABSTRACT: Nanocrystalline $Mg(OH)_2$ was synthesized using four different methods and the crystallite size was calculated from X-ray powder diffraction patterns. For the stabilization of the particles in polymer dispersions, two different surface modifiers were used [poly(N-vinyl-2-pyrrolidone) and 3-methacryloxypropyltrimethoxysilane]. IR spectroscopy measurements show that the surface of the particles is covered with the surface modifiers rendering the particles dispersable in monomer solutions such as butanediol monoacrylate. The dispersions were polymerized into films of 100 μm thickness by addition of a UV initiator (2,4,6-trimethylbenzoyldiphenylphosphine oxide, Lucirin TPO) and a crosslinking agent (trimethylolpropanetriacrylate, Laromer TMPTA) between two glass plates by UV-polymerization. The resulting films were characterized by UV–Vis spectroscopy, thermogravimetry, and scratch resistance tests. © 2010 Wiley Periodicals, Inc. J Appl Polym Sci 116: 2197–2204, 2010

Key words: magnesium hydroxide; acrylates; nanocomposite; microemulsion; scratch resistance; MPTS; PVP

INTRODUCTION

The concept of incorporation of inorganic particles into polymers is an effective method to integrate new functions inside polymer matrices. $Mg(OH)_2$-filled polymers are promising materials due to the low price of the hydroxide and good mechanical properties. As compared with MgO, the hydroxide is beneficial as a flame retardant due to the decomposition into H_2O and MgO at higher temperature. $Mg(OH)_2$ can be obtained in a crystalline form if synthesized properly. As compared with MgO nanoparticles, it is not moisture sensitive and thus easier to store. Numerous investigations on $Mg(OH)_2$ and its properties as flame-retardant inorganic filler material were carried out, because it does not evolve toxic, gaseous, or corrosive substances during decomposition.[1–4]

The integration of an inorganic filler material can affect the mechanical properties of the polymer matrix.[5–8] Inorganic fillers are expected to minimize the scratch damage of polymers, which is advantageous because there is a permanent demand for high surface quality for various applications of polymeric materials. Nanocrystalline $Mg(OH)_2$-powders can be synthesized using different pathways, for example, under solvothermal conditions,[9] in a hydrothermal reaction using different precursors and solvents as reactants,[10–12] or via sol–gel technique.[13,14] One disadvantage of using $Mg(OH)_2$ as filler material is, for example, the large amount that is needed to increase the flame retardant efficiency which leads to a drop of the mechanical properties of the composites.[4,15] This effect can be prevented, for example, by the minimization of the particle size or by surface modification of the particles. The particles often are too hydrophilic to be dispersed in polymers. Attaching organic groups to the surface of the particles should prevent the formation of aggregates and the organophilic surface modification of the inorganic particles (in this case, magnesium hydroxide) should increase the compatibility between the particles and the polymer in order to improve the dispersability and with that the mechanical properties of the composite material.[16,17] Functionalized trialkoxysilanes, for example, are widely used monomers, because of their ability to undergo condensation reactions with surface OH groups.[18,19] Another known grafting agent is poly(N-vinyl-2-pyrrolidone), which is nontoxic and has excellent biocompatible properties.[20–22]

In this work, four different methods were used to produce $Mg(OH)_2$ powders. The powders were synthesized: (a) in ethanol solution, (b) in a microemulsion, (c) with 3-methacryloxypropyltrimethoxysilane (MPTS) in ethanol, and (d) with poly(N-vinyl-2-pyrrolidone) as surface modifier in distilled water as solvent. The preparation of poly(N-vinyl-2-pyrrolidone)-coated $Mg(OH)_2$ was carried out in analogy to a work described by Qiu et al.[23] The different synthesis methods lead to products of different size and

shape. The nature of the powders and crystallite size was examined by X-ray powder diffractometry because it is essential for the particles to be smaller than one-fourth of the wavelength of the incident light to avoid light scattering effects of the particles incorporated into a polymer. Light scattering would lead to decreasing transparency of the polymer/filler composite. To avoid particle aggregation during synthesis or in the polymer dispersions, the two different surface modifying agents were used. They also offer the ability for the modified particle to take part in the polymerization step because a covalent attachment to the polymer matrix is possible, which can be formed by the carbon–carbon double bonds.[17] The synthesis products were dispersed in butanediol monoacrylate (BDMA) with different solid content and polymerized via UV-polymerization after addition of a crosslinking agent (Laromer TMPTA) and UV initiator (Lucirin TPO) between two glass plates.[24] The resulting films were ~ 100 μm thick. The effect of $Mg(OH)_2$ nanocrystallites on the mechanical properties of the polymer was studied via pencil-scratch resistance tests and UV–Vis spectroscopy. The filler content was measured by thermogravimetry.

EXPERIMENTAL

Precipitation in ethanol solutions

For the syntheses in ethanol solution 4.1 g (0.02 mol) $MgCl_2 \cdot 6H_2O$ were dissolved in 200 mL distilled water to a 0.1 molar salt solution. The solution was exposed to an ammonia gas flow of 56 mL/min. The white $Mg(OH)_2$ powder was collected by centrifugation, washed with ethanol, and dried at room temperature.

Precipitation in microemulsions

Marlophen NP5 ($RO(CH_2CH_2O)_xH$, $x = 5$, R = nonylphenyl, $M = 440$ g/mol, SASOL) was chosen as surfactant. The phase diagram was obtained by adding the surfactant to mixtures of n-heptane (>99%, Aldrich) and deionized water under vigorous stirring at 20°C until the microemulsions appear transparent (Fig. 1). The equilibration time was 15 min. The reverse microemulsions were set aside to verify that phase separation would not occur after stirring was stopped. All microemulsions remained stable for at least 24 h.

The aqueous phase of the microemulsions contained a 2 molar salt solution of $MgCl_2 \cdot 6H_2O$. The composition of the microemulsion used for $Mg(OH)_2$ synthesis was as follows: 4 g (0.04 mol) heptane, 0.5 mL of a 2 molar $MgCl_2$ salt solution, and 1.2 g (0.003 mol) Marlophen NP5. The reverse microemulsion
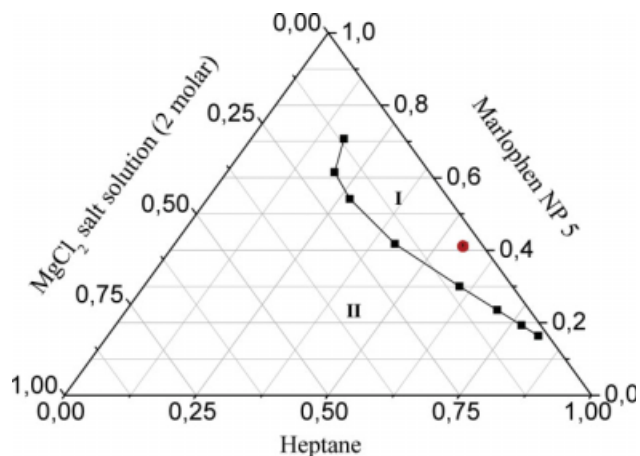
Figure 1 Oil-rich region of the phase diagram for Marlophen NP5/heptane/water with solutes in the aqueous phase (I = isotropic solution, II = two phase region, x = mass fraction). The solid circle marks the composition of the microemulsion used for $Mg(OH)_2$ synthesis. [Color figure can be viewed in the online issue, which is available at www.interscience.wiley.com.]

appeared transparent after stirring. The reverse microemulsion was characterized by DLS using a Zetasizer Nano ZS from Malvern Instruments. The micelle size was measured at 20°C. For DLS measurements, the viscosity of the solvent was used. The average particle diameter (z-average) was determined from intensity weighed size distributions, calculated using the NNLS-algorithm.

The micelle size was measured as 13.4 nm z-average (PDI 0.05). The microemulsion was exposed to an ammonia gas flow of 56 mL/min, the white precipitate was isolated by centrifugation, washed with ethanol, and dried at room temperature.

Synthesis of surface-modified $Mg(OH)_2$ nanocrystallites with poly(N-vinyl-2-pyrrolidone)

In the synthesis, 20.0 g $MgCl_2 \cdot 6H_2O$, 1.0 g potassium oleate, and 0.25 g Poly(N-vinyl-2-pyrrolidone) were simultaneously dissolved in 30.0 g distilled water. The solution was stirred for 1 h at room temperature. An alkaline solution of 2 mol/L NaOH was added until the pH value 10 was reached. The suspension obtained was allowed to age for 1 h at room temperature under vigorous stirring. The $Mg(OH)_2$ powder was collected, washed with distilled water, and dried at room temperature.

Synthesis of surface-modified $Mg(OH)_2$ nanoparticles with 3-methacryloxypropyltrimethoxysilane

In a typical synthesis, 2.03 g (0.01 mol) $MgCl_2 \cdot 6H_2O$ and 4.96 g (0.02 mol) with MPTS were dissolved in 100 mL ethanol. Although being treated in an

TABLE I
Compositions of the Acrylate Films

Filler material	Solid content (%, g)	BDMA (g)	TMPTA (g)	Lucirin TPO (g)
MPTS modified	3, 0.09	2.5	0.62	0.09
MPTS modified	6, 0.19	2.5	0.62	0.09
MPTS modified	9, 1.28	2.5	0.62	0.09
PVP modified	3, 0.09	2.5	0.62	0.09
PVP modified	6, 0.19	2.5	0.62	0.09
PVP modified	9, 0.28	2.5	0.62	0.09
Ethanolic solution	3, 0.09	2.5	0.62	0.09
Ethanolic solution	6, 0.19	2.5	0.62	0.09
Ethanolic solution	9, 0.28	2.5	0.62	0.09
Microemulsion	3, 0.09	2.5	0.62	0.09
Microemulsion	6, 0.19	2.5	0.62	0.09
Microemulsion	9, 0.28	2.5	0.62	0.09
Without filler	–	2.5	0.62	0.09

ultrasonic bath, 1.5 mL of a 13.3 molar solution of ammonia in water were added to the solution. The obtained turbid solution was kept under ultrasound for 1 h at room temperature. The white powder was isolated by centrifugation, washed with ethanol, and dried at room temperature.

Preparation and polymerization of acrylate-mixtures with various filler content and polymerization as films

The $Mg(OH)_2$ powders were diluted with BDMA and ultrasound for 60 min and milky dispersions were obtained. These dispersions were stable for a few hours but sedimentation occurred. In case of the surface-modified samples, the dispersions were stable for days and there was only little sedimentation observed. To prepare polymer films with a thickness of 100 μm, the suspensions were mixed with TMPTA and Lucirin TPO (Table I). The mixture was filled in between two glass plates separated by double faced adhesive tape (width 50 mm, length 25 m), Scheme 1. Polymerization was carried out in a UV cube inert (Hoenle AG) using UV radiation (200 W/cm, LAMP FOZFR 100 D22 U150 E3S9) for 10 min.

X-ray diffraction analysis

X-ray diffraction (XRD) powder patterns were recorded in transmission geometry using a Stoe Stadi-P diffractometer and Cu $K\alpha_1$ radiation ($\lambda = 0.15405$ nm). For crystallite size determinations, the single-line size/strain analysis (WinXPow, Stoe) was used.

IR spectroscopy

The samples were prepared for IR spectroscopy in KBr-Pellets. The spectrometer used was a BioRad

Excalibur Series IR-spectrometer FTS 3000 (wavenumber interval: 4000 cm^{-1} to 400 cm^{-1}, scans: 64, resolution: 4 cm^{-1}).

### Thermogravimetric analysis of the surface-modified $Mg(OH)_2$ and on the polymer films

Thermogravimetric measurements were performed by heating the sample at 5°C/min using a device from Netzsch (simultaneous thermal analysis, TG and DTA/DSC, STA 409) to quantify the residual mass by combustion of the sample.

UV–Vis spectroscopy

The UV–Vis measurements were carried out using a UV-1650 PC spectrometer (Shimadzu). The transmission was measured from 800 nm to 200 nm without using cuvettes; the 100-μm-thick polymer films were placed and fixed in front of the light beam.

Scratch resistance of the composite materials

The scratch tests were done using a pencil-scratch hardness testing device according to Wolff-Wilborn Model 291. In this method, pencils of various grades of hardness were moved over the surface that was to be tested. The angle between pencil and surface was 45° to the horizontal and the testing device was moved with a force of 7.5 N. The pencil hardness of the surface was defined by those two grades of hardness: the softer one of which just produced a writing trace, whereas the next harder one gave a perceptible scratch on the surface. An assortment of pencils with 17° of hardness from 6 B to 9 H was used for testing. The pencil with 6 B was the softest, whereas the pencil with 9 H was the hardest one. The scratch resistance was measured on polymer films. The films were fixed on a glass substrate for measurement.
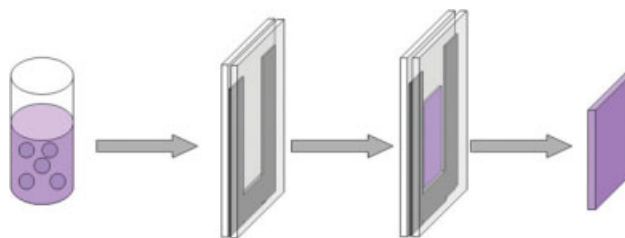
Scheme 1 Reaction setup for polymerization with glass chamber and spacer. [Color figure can be viewed in the online issue, which is available at www.interscience.wiley.com.]
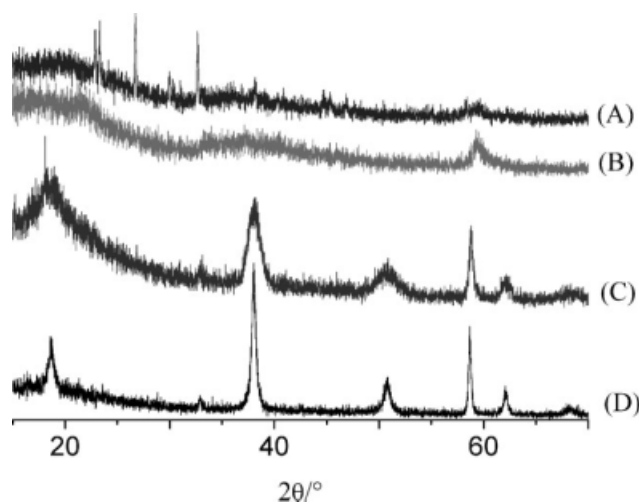
Figure 2 XRD-patterns of $Mg(OH)_2$ synthesized via different methods with and without surface modification.

RESULTS AND DISCUSSION

### X-ray diffraction analysis and microscopy

The powder XRD pattern of the surface-modified $Mg(OH)_2$ powder with MPTS showed amorphous characteristics [Fig. 2(A)]. Some sharp reflections of low intensity indicate the presence of an unidentified crystalline side product. The pattern of the powder synthesized in ethanol solution also showed a strong amorphous character [Fig. 2(B)]. All reflections in Figure 2(C,D) correspond to crystalline magnesium hydroxide. $Mg(OH)_2$ surface modified with poly(N-vinyl-2-pyrrolidone) showed no XRD reflections arising from impurities. The reflections of the measured sample were significantly broadened [Fig. 2(C)]. This indicates the small grain size of the $Mg(OH)_2$ crystallites. The crystallite size was calculated from the broadened XRD reflections with the Scherrer equation. As a result, the size of 25.6 nm was obtained. The reflections of the sample synthesized in microemulsion were broadened and no impurities could be seen [Fig. 2(D)]. The crystallite size was calculated as 20.5 nm. Scanning electron micrographs (Fig. 3) reveal the very fine nanostructure of the $Mg(OH)_2$ nanoparticles. A dominant morphological feature seen in the SEM is the plate-like morphology [Fig. 3(B,D)] of the particles. Only MPTS modified particles show a more granular particle structure. The particles are highly aggregated after isolation as a powder.

IR spectroscopy

Evidence for the presence of the surfactant PVP onto the surface of the $Mg(OH)_2$ particles was obtained using FTIR spectroscopy [Fig. 4(A)]. The reflections at 2927 cm^{-1} and 2852 cm^{-1} show the asymmetric and symmetric vibrations of aliphatic groups $(-CH_2-)_n-$.[23] This indicates that the surfactants are adsorbed onto the surface of the $Mg(OH)_2$ particles. A contribution
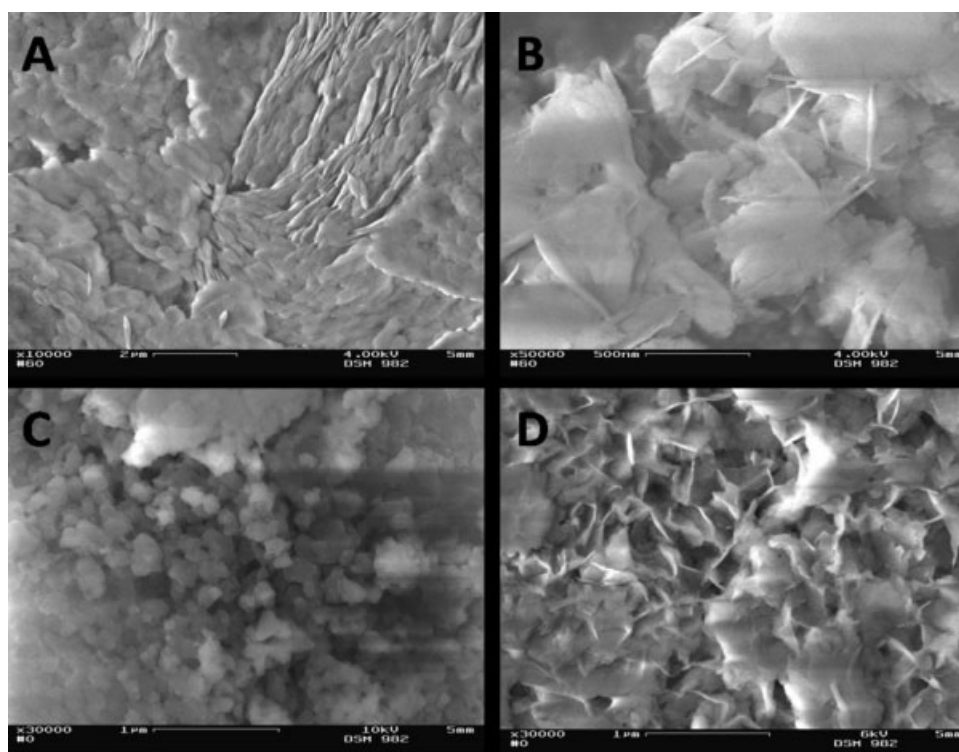
Figure 3 Scanning electron micrographs (A) microemulsion derived $Mg(OH)_2$, (B) from ethanol, (C) MPTS modified, and (D) PVP modified.
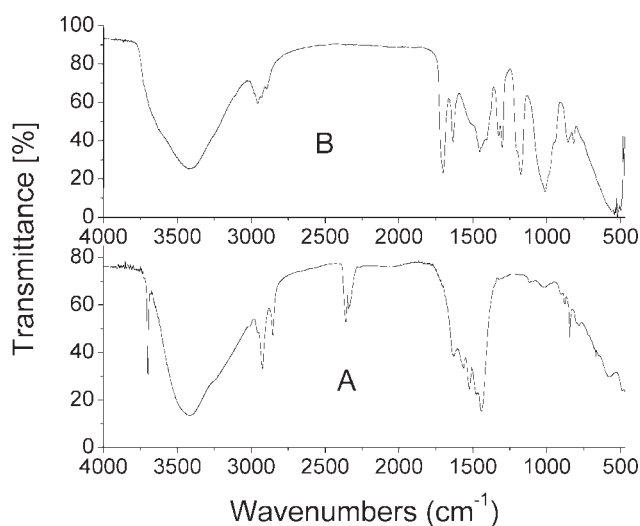
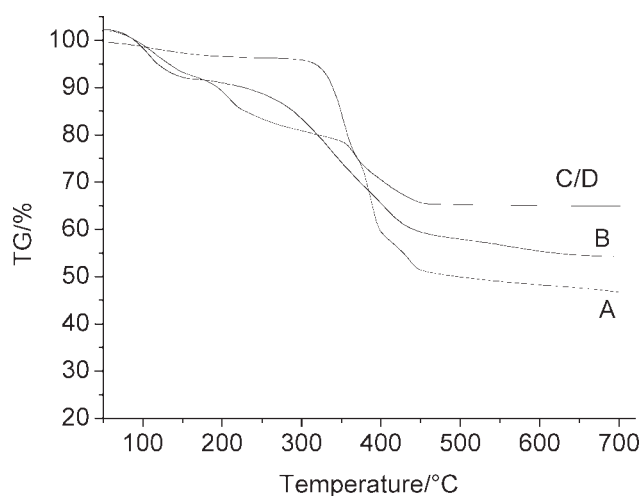**Figure 4** FTIR-spectrum of (A) Mg(OH)$_2$ modified with PVP and (B) MPTS after drying at room temperature.

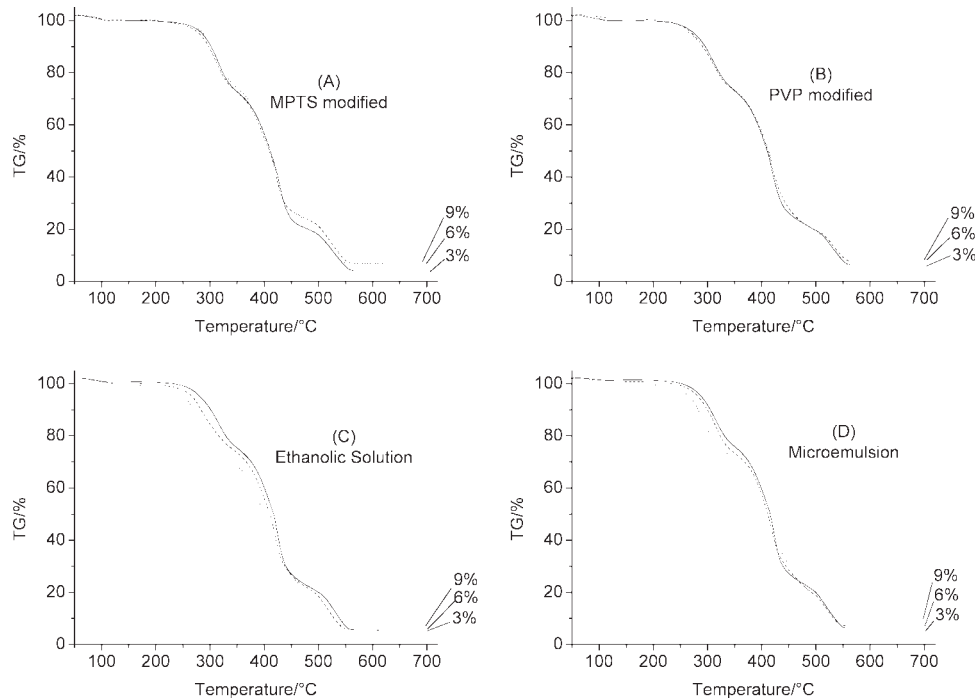

Figure 5 Thermogravimetric measurements on Mg(OH)$_2$ modified with (A) PVP, (B) MPTS, (C) without surface modification from ethanol solution, and (D) microemulsion.

from solvent molecules to the IR absorption is less likely because the samples were dried before analysis. The sharp peak at 3701 cm^{-1} can be assigned to the OH-stretching band in the crystal structure. The absorption reflections at 1620–1444 cm^{-1} can be associated to the OH bending mode of water or the CH$_2$/NH scissoring mode of the surfactant PVP. The surface-modified particles with MPTS were also investigated [Fig. 4(B)].[25] The reflections at 2927 cm^{-1} and 2852 cm^{-1} show the asymmetric and symmetric vibrations of aliphatic groups (—CH$_2$—)$_n$—. The bands close to 1713 cm^{-1} and 1632 cm^{-1} are associated to the stretching vibrations of C=O and C=C groups, respectively. The absorption bands located at 1327 cm^{-1} and 1299 cm^{-1} are assigned to the C—O—C bonds and wagging vibration of CH$_3$ groups of the MPTS molecule. The band at 1180 cm^{-1} is attributed to stretching vibrations of Si—O—C bonds and the broad peak around 1002 cm^{-1} is assigned to bending vibrations of these Si—O—C bonds. This indicates that MPTS is adsorbed on the surface of the Mg(OH)$_2$ particles. IR spectroscopy alone can often not clearly distinguish between adsorbed modifiers or a physical mixture of the modifier and the particle. However, the use of the modifier leads to a significant improvement of the particle dispersion in monomers (below) also indicating adsorption on the particle surface.

The IR spectra are also in agreement with a physical mixture of the modifier and the particles. The strong band at 530 cm^{-1} is attributed to the MgO stretching vibration in Mg(OH)$_2$.

Thermogravimetric analysis of the surface-modified magnesium hydroxide

The surface-modified Mg(OH)$_2$ products were investigated by thermogravimetry (Fig. 6). The hydroxide

coated with PVP decomposes to a residual mass of 43.01 wt % at 700°C, that is, due to resulting MgO. The dehydration of the hydroxide starts at 365°C. The change in the mass of the sample between 100°C and 700°C is associated with the decomposition of the organic coating and to the decomposition of the hydroxide to magnesium oxide [Fig. 5(A)]. The sample coated with MPTS shows a residual mass of 50.69 wt % at 700°C, which can be assigned to MgO and SiO$_2$ resulting from the decomposition of MPTS and dehydration of Mg(OH)$_2$ which starts at 260°C [Fig. 5(B)]. The powder prepared from ethanol MgCl$_2$ solution showed a residual mass of 64.9 wt % [Fig. 5(C)] after thermal decomposition and for the sample precipitated in microemulsion a residual mass of 63.9 wt % was measured [Fig. 5(D)]. The decomposition of the hydroxide to magnesium oxide starts for both samples at 350°C.

TABLE II
TGA-Analysis of the Mg(OH)$_2$ Filled Polymer Films

Films	Solid content (%, g)	Residual mass at 700°C (%)
MPTS modified	3, 0.09	0.95
MPTS modified	6, 0.19	3.37
MPTS modified	9, 1.28	3.30
PVP modified	3, 0.09	3.16
PVP modified	6, 0.19	4.30
PVP modified	9, 0.28	3.60
Ethanolic solution	3, 0.09	1.89
Ethanolic solution	6, 0.19	2.31
Ethanolic solution	9, 0.28	3.30
Microemulsion	3, 0.09	3.28
Microemulsion	6, 0.19	3.64
Microemulsion	9, 0.28	4.95
Without filler	–	1.18

Figure 6 Thermogravimetric measurements on acrylate films with Mg(OH)$_2$ modified with (A) MPTS and (B) PVP and without surface modification from (C) ethanol solution and (D) microemulsion with different solid content.
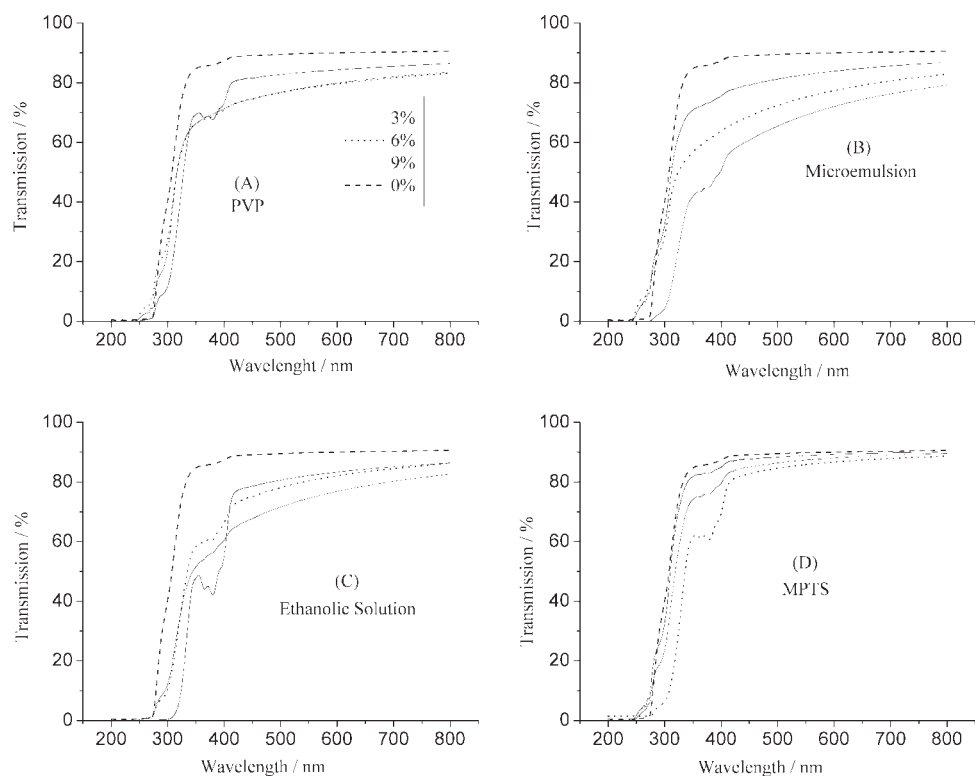
Figure 7 UV–Vis transmission spectra of acrylate films containing different Mg(OH)$_2$ powders (A) PVP, (B) from microemulsion, (C) from ethanol solution, and (D) with MPTS and with different solids content.

TABLE III
Transmittance of the Composite-Films with Mg(OH)$_2$ from Different Syntheses with Different Solid Content in % at 700 nm

| Solid content (wt %)	Mg(OH)$_2$ from ethanol solution	Mg(OH)$_2$ from microemulsion	Mg(OH)$_2$ modified with MPTS	Mg(OH)$_2$ modified with PVP
0	90.0	90.0	90.0	90.0
3	86.4	86.7	89.0	86.4
6	86.0	82.5	87.6	83.0
9	82.6	80.0	86.4	83.5

Film characterization

Different types of Mg(OH)$_2$-filled films were prepared and they were examined by UV–Vis spectrometry, thermogravimetry, and scratch resistance measurements.

Four films were prepared with the same content (wt %), but different filler material and three films with different content, but the same filler. To measure the filler content of the polymer films, thermogravimetry was used (Table II). The reference polymer without Mg(OH)$_2$ decomposed to a residual mass of 1.18% at 700°C. The latter leads to the conclusion that the polymer is almost completely decomposed. In case of not modified Mg(OH)$_2$, the residual mass at 700°C is assigned to MgO resulting from decomposition of the hydroxide. The resulting products after decomposition of the films with the surface-modified Mg(OH)$_2$ sample coated with MPTS are MgO and SiO$_2$. The major decomposition product of the films filled with hydroxide with PVP on the surface should be MgO. The residual masses at 700°C of the films filled with the different hydroxide powders are lower than the original amount dispersed in the monomer. This weight loss is due to the fact that the filler before decomposition was Mg(OH)$_2$ with and without MPTS or PVP on the surface, and after the process, the resulting solid product was MgO and for the MPTS modified sample also SiO$_2$.

Transmission spectra were measured for 100-μm-thick polymer samples. The transmission spectrum of the pure polymer shows a high transmittance in the visible spectral range of 90% at 700 nm (Fig. 7). In comparison with the spectrum of the pure polymer, the spectra of the polymer/Mg(OH)$_2$ composites showed lower transmittance in the visible (Table II). The loss of transmittance can be attributed to light scattering by particles. The spectra of the polymer composites with Mg(OH)$_2$ particles, which were generated under different synthesis conditions; all show the tendency of decreasing transmission with increasing filler content down to 80% transmission in the visible with 9 wt % filler from microemulsion synthesis (Table III). The slightly reduced transmission is caused by the formation of aggregates or incomplete dispersion. The transmission values of the Mg(OH)$_2$ filled polymer films are high considering the thickness of 100 μm.

For pencil-scratch resistance measurements, the films were fixed on a glass substrate for measurement. The pure polymer film shows a scratch resistance of H/2H. The scratch resistance increases with increasing filler content up to 4H/5H for a sample filled with 9 wt % Mg(OH)$_2$ modified with MPTS and for a sample filled with 9 wt % hydroxide from synthesis in ethanol solution. An increase up to 3H/4H was observed for films filled with Mg(OH)$_2$ synthesized from microemulsion or modified with PVP (Fig. 8).
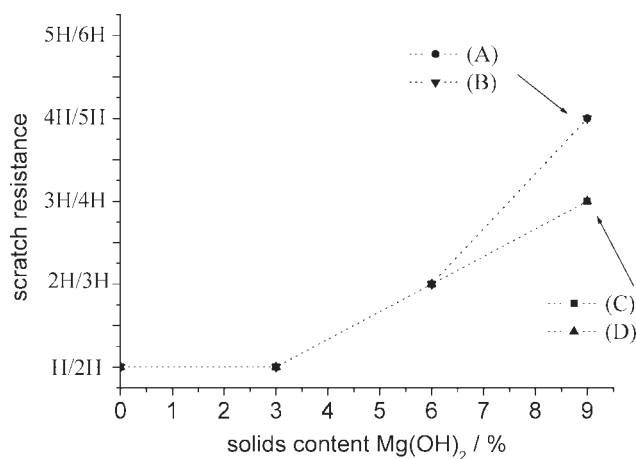
Figure 8 Pencil-scratch resistance of the polymer films with Mg(OH)$_2$ filler from different syntheses with different solids content: films filled with hydroxide from (A) ethanol solution, (B) coated with MPTS, (C) from microemulsion, and (D) coated with PVP.

CONCLUSIONS

Nanocrystalline Mg(OH)$_2$ was produced via four different syntheses methods with and without surface modification. For surface modification of the particles, MPTS and poly(N-vinyl-2-pyrrolidone) were used. The crystallite size calculated applying

the Scherrer equation was between 16 nm and 26 nm, and the powders prepared by precipitation in ethanol with and without MPTS show amorphous character. The interpretation of IR-spectra of the synthesis products with MPTS and PVP leads to the conclusion that the particles were successfully surface modified. The dispersability of the particles in BDMA increases with surface modification. Using a photo initiator and a crosslinker, the $Mg(OH)_2$ dispersions can be polymerized by UV initiation as films with 100 μm thickness. They show high transmittance values exceeding 80% with 9 wt % filler content, which is very high considering the 100 μm thickness of the films. The scratch resistance increases significantly in the $Mg(OH)_2$/polymer nanocomposite films as compared with the pure polymer films.

References

1. Mishra, S.; Sonawane, S. H.; Singh, R. P.; Bendale, A.; Patil, K. J Appl Polym Sci 2004, 94, 116.
2. Sain, M.; Park, S. H.; Suhara, F.; Law, S. Polym Degrad Stab 2004, 83, 363.
3. Chiu, S. H.; Wang, W. K. J Appl Polym Sci 1998, 67, 989.
4. Wang, J.; Tung, J. F.; Fuad, M. Y. A.; Hornsby, P. R. J Appl Polym Sci 1996, 60, 1425.
5. Henrist, C.; Mathieu, J. P.; Vogels, C.; Rulmont, A.; Cloots, R. J Cryst Growth 2003, 249, 321.
6. Althues, H.; Henle, J.; Kaskel, S. Chem Soc Rev 2007, 36, 1454.
7. Althues, H.; Simon, P.; Kaskel, S. J Mater Chem 2007, 17, 758.
8. Du, H. C.; Wohlrab, S.; Weiss, M.; Kaskel, S. J Mater Chem 2007, 17, 4605.
9. Fan, W. L.; Sun, S. X.; You, L. P.; Cao, G. X.; Song, X. Y.; Zhang, W. M.; Yu, H. Y. J Mater Chem 2003, 13, 3062.
10. Ding, Y.; Zhang, G. T.; Wu, H.; Hai, B.; Wang, L. B.; Qian, Y. T. Chem Mater 2001, 13, 435.
11. Li, Y. D.; Sui, M.; Ding, Y.; Zhang, G. H.; Zhuang, J.; Wang, C. Adv Mater 2000, 12, 818.
12. Yan, L.; Zhuang, J.; Sun, X. M.; Deng, Z. X.; Li, Y. D. Mater Chem Phys 2002, 76, 119.
13. Utamapanya, S.; Klabunde, K. J.; Schlup, J. R. Chem Mater 1991, 3, 175.
14. Ranjit, K. T.; Klabunde, K. J. Chem Mater 2005, 17, 65.
15. Wang, Z. Z.; Qu, B. J.; Fan, W. C.; Huang, P. J Appl Polym Sci 2001, 81, 206.
16. Kaskel, S. Kunststoffe 2006, 96, 36.
17. Zhou, S. X.; Garnweitner, G.; Niederberger, M.; Antonietti, M. Langmuir 2007, 23, 9178.
18. Daniels, M. W.; Francis, L. F. J Colloid Interface Sci 1998, 205, 191.
19. Beari, F.; Brand, M.; Jenkner, P.; Lehnert, R.; Metternich, H. J.; Monkiewicz, J.; Siesler, H. W. J Organomet Chem 2001, 625, 208.
20. Voronov, A.; Kohut, A.; Synytska, A.; Peukert, W. J Appl Polym Sci 2007, 104, 3708.
21. Inoue, H.; Kohama, S. J Appl Polym Sci 1984, 29, 877.
22. Heffernan, J. G.; Sherrington, D. C. J Appl Polym Sci 1984, 29, 3013.
23. Qiu, L. Z.; Xie, R. C.; Ding, P.; Qu, B. J. Compos Struct 2003, 62, 391.
24. Althues, H.; Simon, P.; Philipp, F.; Kaskel, S. J Nanosci Nanotechnol 2006, 6, 409.
25. Nassar, E. J.; Nassor, E. C. D.; Avila, L. R.; Pereira, P. F. S.; Cestari, A.; Luz, L. M.; Ciuffi, K. J.; Calefi, P. S. J Sol-Gel Sci Technol 2007, 43, 21.